Elastic properties of vanadium-based alloys from first-principles theory

Xiaoqing Li,[1,*] Hualei Zhang,[1] Song Lu,[1] Wei Li,[1] Jijun Zhao,[2,3,*] Börje Johansson,[1,4] and Levente Vitos[1,4,5]

[1]*Applied Materials Physics, Department of Materials Science and Engineering, Royal Institute of Technology, Stockholm SE-10044, Sweden*

[2]*School of Physics and Optoelectronic Technology and College of Advanced Science and Technology, Dalian University of Technology, Dalian 116024, China*

[3]*Key Laboratory of Materials Modification by Laser, Electron, and Ion Beams (Dalian University of Technology), Ministry of Education, Dalian 116024, People's Republic of China*

[4]*Department of Physics and Astronomy, Division of Materials Theory, Box 516, SE-75120 Uppsala, Sweden*

[5]*Research Institute for Solid State Physics and Optics, Wigner Research Center for Physics, P.O. Box 49, Budapest H-1525, Hungary*

(Received 10 February 2012; published 10 July 2012)

The effect of Cr and Ti on the fundamental mechanical properties of V-Cr-Ti alloys has been investigated using the all-electron exact muffin-tin orbitals method in combination with the coherent-potential approximation. The static lattice constant and elastic parameters have been calculated for the body-centered-cubic $V_{1-x-y}Cr_xTi_y$ ($0 \leqslant x,y \leqslant 0.1$) random solid solution as a function of composition. Our theoretical predictions are in good agreement with the available experimental data. Alloys along the equicomposition region are found to exhibit the largest shear and Young's modulus as a result of the opposite alloying effects obtained for the two cubic shear elastic constants. The classical solid-solution hardening (SSH) model predicts larger strengthening effect in $V_{1-y}Ti_y$ than in $V_{1-x}Cr_x$. By considering a phenomenological expression for the ductile-brittle transition temperature (DBTT) in terms of Peierls stress and SSH, it is shown that the present theoretical results can account for the variations of DBTT with composition.

DOI: 10.1103/PhysRevB.86.014105 PACS number(s): 71.20.Be, 62.20.−x, 61.50.−f, 71.15.Nc

I. INTRODUCTION

Vanadium alloys are identified as leading candidate materials for fusion first-wall/blanket structure applications. This is because some vanadium alloys exhibit superior mechanical properties, decent thermal creep behavior, high thermal conductivity, good resistance to irradiation-induced swelling and damage, and long operating lifetime in the fusion environment.[1–6] Considerable efforts have been made to find optimal V-based alloy compositions that can endure the extreme environments of fusion reactors.

The available experimental data indicate that reasonable properties can be achieved by introducing a few percent Ti and Cr into the V matrix.[1,7] Consequently, the vanadium-chromium-titanium (V-Cr-Ti) system has attracted a broad interest, and in particular the compositions with 0–15 at.% Cr and 0–20 at.% Ti have been intensively investigated.[4,8–19] Previous studies on V-Cr-Ti alloys were mainly focused on the ductile-brittle transition temperature (DBTT) before and after irradiation, swelling properties, and impact toughness as a function of Cr and Ti contents. For example, Chuang *et al.*[1] found that V-Cr-Ti alloys have low DBTT if the total concentration of Cr and Ti is lower than 10 at.%, while DBTT firmly increases when further Cr and Ti are added to the alloy. Matsui *et al.*[2] investigated the behavior of V-4Cr-4Ti, V-10Cr-5Ti, and V-15Cr-5Ti alloys after irradiation and reported that the V-4Cr-4Ti alloy exhibits excellent resistance to irradiation-induced swelling, that is, even at irradiation up to 30 dpa at 600 °C the swelling still remained below 0.4%.

It is well known that the elastic properties of materials can be used to characterize their mechanical deformation and structural stability under external loading.[20,21] For example, the shear modulus (G) is generally considered as an indicator of the mechanical characteristics for a large set of materials,[22] and the bulk modulus (B) is used to unveil the average bond strength. In addition to elastic behavior, the ratio of bulk modulus and shear modulus (B/G) is often employed to assess the ductile/brittle characteristics of materials.[23,24] To our knowledge, most experimental efforts on V-Cr-Ti alloys have been devoted to the effect of Cr and Ti contents on irradiation behaviors and DBTT. Little attention has been paid to the effect of Cr and Ti on the fundamental mechanical properties of V-Cr-Ti alloys, such as the elastic and misfit parameters, and the ductile/brittle behavior, which could guide further optimization of the composition of V-based alloys. In this work, we employ *ab initio* alloy theory to investigate the above bulk properties of the body-centered-cubic (bcc) $V_{1-x-y}Cr_xTi_y$ random alloys as a function of Cr ($0 \leqslant x \leqslant 0.1$) and Ti ($0 \leqslant y \leqslant 0.1$) concentrations.

The structure of the paper is as follows. In Sec. II, we describe the computation tool and the most important numerical details. The results are presented and discussed in Sec. III. First we assess the accuracy of our calculations, then study the trends obtained for the bulk properties and finally use the calculated parameters to explain the experimental DBTT maps.

II. COMPUTATIONAL METHOD

A. Total energy calculation

All calculations were performed using the exact muffin-tin orbitals (EMTO) method[25–27] based on density functional theory (DFT)[28] and the Green's function and full charge density techniques. The self-consistent calculations were carried out using the local density approximation (LDA)[29] to describe the exchange-correlation potential and for the total energy we adopted the generalized gradient approximation formulated via the Perdew-Burke-Ernzerhof (PBE)[30] functional. This LDA-PBE scheme suits very well the full charge density

formalism[31] and has been shown to produce errors in the equation of state which are within the numerical accuracy of common DFT calculations.[32,33] The problem of disorder was treated within the coherent-potential approximation (CPA).[34–37] We mention that since CPA is a single-site approximation, the present study cannot account for the short range order and local relaxation effects. Therefore, all our results are strictly valid for completely disordered alloys with rigid underlying bcc crystal structure.

The EMTO method is an improved screened Korringa-Kohn-Rostoker (KKR) method,[25] where the full potential is represented by overlapping muffin-tin potential spheres. Inside these spheres, the potential is spherically symmetric and constant in between. By using overlapping spheres, one describes more accurately the exact crystal potential compared to the conventional muffin-tin or nonoverlapping methods.[26,38] Further details about the EMTO method and its self-consistent implementation can be found in previous works.[25–27,36,37] The accuracy of the EMTO method for the equation of state and elastic properties of metals and alloys has been demonstrated in a number of works.[26,35,39–43]

B. Details of numerical calculations

The elastic properties of single-crystals can be described by the elements C_{ij} of the elasticity tensor. For cubic crystal, there are three independent parameters: C_{11}, C_{12}, and C_{44}. They are connected to the tetragonal shear modulus $C' = (C_{11} - C_{12})/2$ and the bulk modulus $B = (C_{11} + 2C_{12})/3$.

In the present study, the cubic elastic constants of $V_{1-x-y}Cr_xTi_y$ were calculated as a function of chemical composition. For each concentration, the equilibrium lattice parameter and the bulk modulus of $V_{1-x-y}Cr_xTi_y$ were determined from an exponential Morse-type function,[44] which was fitted to the *ab initio* total energies calculated for seven different atomic volumes. To obtain the two cubic shear modulus C' and C_{44}, volume-conserving orthorhombic and monoclinic deformations were applied on the conventional cubic cell.[45] For tetragonal shear modulus C', the following orthorhombic deformation was used:

$$\begin{bmatrix} 1+\delta_0 & 0 & 0 \\ 0 & 1-\delta_0 & 0 \\ 0 & 0 & 1/(1-\delta_0^2) \end{bmatrix},$$

which leads to the energy change

$$\Delta E(\delta_0) = 2VC'\delta_0^2 + O(\delta_0^4). \quad (1)$$

The C_{44} shear modulus was determined from the monoclinic distortion

$$\begin{bmatrix} 1 & \delta_m & 0 \\ \delta_m & 1 & 0 \\ 0 & 0 & 1/(1-\delta_m^2) \end{bmatrix},$$

yielding

$$\Delta E(\delta_m) = 2VC_{44}\delta_m^2 + O(\delta_m^4), \quad (2)$$

where δ is the strain parameter. We considered six distortions $\delta = 0.00, 0.01, \ldots, 0.05$. To obtain the accuracy needed for the calculation of the elastic constants, we used 20 000–27 000 k points, depending on the particular distortion, in the irreducible wedge of the Brillouin zones.

TABLE I. Theoretical and experimental equilibrium lattice parameter (a in Å) and single-crystal elastic constants (C_{ij} in GPa) for bcc V. The present results (EMTO) are compared to former theoretical (PAW, Ref. 49; LAPW, Ref. 51; FP-LMTO, Ref. 50) and experimental (Ref. 48) data.

	Method	a	C_{11}	C_{12}	C'	C_{44}
Theory	EMTO	2.998	281.72	124.63	78.54	36.09
	PAW	2.990	268.30	130.30	69.00	51.00
	LAPW		205.00	111.00	62.50	30.00
	FP-LMTO		205.00	130.00	37.50	5.00
Experiment	4.2 K	3.030	237.00	121.00	58.00	47.00
	270 K		231.65	120.03	55.68	44.03
	300 K		230.98	120.17	55.40	43.77

From the single-crystal elastic constants, the polycrystalline shear modulus (G) can be obtained by the arithmetic Hill average[46] $G_H = 1/2(G_R + G_V)$, where the Reuss and Voigt bounds[37] are

$$G_R^{-1} = 2/5C'^{-1} + 3/5C_{44}^{-1} \quad (3)$$

and

$$G_V = 2/5C' + 3/5C_{44}. \quad (4)$$

For cubic solids, the polycrystalline bulk modulus is equivalent with the single-crystal one. The Young's modulus (E) and the Poisson ratio (ν) can be expressed as $E = 9BG/(3B + G)$ and $\nu = (3B - 2G)/(6B + 2G)$. The longitudinal ($\upsilon_L$) and the transversal ($\upsilon_T$) sound velocities are obtained from the polycrystalline elastic moduli,[47] viz.

$$\rho\upsilon_L^2 = B + \tfrac{4}{3}G \quad \text{and} \quad \rho\upsilon_T^2 = G, \quad (5)$$

where ρ is the density. The average sound velocity

$$\upsilon_m^{-3} = \frac{1}{3}\left(\frac{1}{\upsilon_L^3} + \frac{2}{\upsilon_T^3}\right) \quad (6)$$

determines the elastic Debye temperature according to

$$\Theta_D = \frac{h}{k_B}\left(\frac{3}{4\pi V}\right)^{1/3}\upsilon_m, \quad (7)$$

where V is the average atomic volume, h is Planck's constant, and k_B is Boltzmann's constant.

III. RESULTS AND DISCUSSION

A. Bulk parameters of pure vanadium

In Tables I and II, we compare the theoretical equilibrium lattice constant, single-crystal elastic constants, polycrystalline elastic moduli, and Debye temperature of pure vanadium with the corresponding experimental data[48] and a few previous theoretical predictions.[49–51] All present elastic parameters were calculated for the theoretical equilibrium lattice parameter. The lattice parameter calculated by us agrees well with the one by projector augmented wave (PAW) method using the GGA-PW91 functional.[49] Comparing to the experimental data,[48] the above theoretical values deviate

TABLE II. Theoretical and experimental polycrystalline elastic constants (in GPa), B/G ratio, Poisson' ratio (ν), and Debye temperature (Θ, in K) for bcc V. The present results (EMTO) are compared to former theoretical (PAW, Ref. 49; LAPW, Ref. 51; FP-LMTO, Ref. 50) and experimental (Ref. 48) data.

	Method	B	G	B/G	E	ν	Θ
Theory	EMTO	176.99	49.56	3.57	135.98	0.372	396.4
	PAW	176.30	58.20	3.03	157.30	0.350	
	LAPW	142.33	36.80	3.86	101.64	0.381	
	FP-LMTO	155.00	18.00	8.60	51.98	0.440	
Experiment	4.2 K	157.02	51.40	3.06	139.03	0.352	404.0
	270 K	157.41	48.69	3.23	132.53	0.361	
	300 K	157.12	48.22	3.26	131.23	0.361	

only by 1%. The elastic constants C_{12} and C_{44} of bcc V are accurately reproduced by our method, while C_{11} and C' are somewhat overestimated. Repeating the EMTO calculation for C' at the experimental volume, we obtained $C' = 71$ GPa, which indicates that the volume effect (partly due to thermal expansion neglected in the present study and partly to the basic density functional error) can account for about 35% of the EMTO error for C'. The shear modulus (G), Young's modulus (E), Poisson's ratio (ν), and Debye temperature (Θ) (Table II) agree within 9%, 2%, 6%, and 2%, respectively, with the corresponding experimental values.

B. Assessing the accuracy of the theoretical predictions for alloys

To assess the reliability of our computational approach for alloys, we first compare the present elastic parameters calculated for binary V-based alloys with the available experimental data (Fig. 1). For binary V-Cr and V-Ti alloys, the theoretical lattice constants increase (decrease) with increasing Ti (Cr) concentration. Furthermore, the bulk modulus and the tetragonal shear elastic constant increase (decrease) with Cr (Ti) addition. These theoretical predictions agree well with the trends observed in experiments (Fig. 1, six upper panels).[52–56] At the same time, the theoretical C_{44} shows small negative (positive) change with Cr (Ti) addition to V, whereas for V-Cr (V-Ti) the experimental variation of C_{44} is slightly positive (negative).[53,56] We return to the theoretical trends obeyed by C_{44} in Sec. III C 2. The discrepancies become even more pronounced when comparing the theoretical and the experimental trends for the shear modulus versus composition (Fig. 1, lower panels). While theory predicts decreasing G for both V-Cr and V-Ti with increasing doping level, experiments reported increasing shear modulus upon alloying V with either Cr or Ti.[53,56]

The above deviations between theory and experiment call for a detailed investigation. Numerous previous applications confirm the accuracy of the EMTO approach for the elastic properties of random solid solutions, and there is no *a priori* reason why it should perform less accurately for the present V-based binary alloys either. The theoretical results correspond to static conditions (0 K), and temperature might change the compositional trends to some extent. This is a question to be investigated in the future. On the other hand, as we demonstrate below, the quoted experimental values for G may not correspond to random solid solutions (as assumed in the present calculations) and are inconsistent with the single-crystal data. The first problem is related the miscibility gap in the V-Ti system below ~900 K. According to that, the experiments on V-27%Ti and V-47%Ti were performed either on quenched (metastable) or on decomposed samples. We note that since the present calculations correspond to completely disordered phase (modeled by the CPA), future theoretical investigations taking into account the local ordering and relaxation effects are needed be able to answer the above question.

The second concern is the inconsistency between the measured single-crystal and the polycrystalline data. For V-Ti, it was reported that both C_{44} and C' decrease and G increases with the amount of Ti. However, according to the Voigt and Reuss models [see Eqs. (3) and (4)], when both C_{44} and C' decrease the shear modulus should also decrease and vice versa. One might argue that the Voigt and Reuss bounds give upper and lower values, respectively, and the true shear modulus might still change within these limits. However, V and V-27%Ti (assuming a random solid solution model) are especially isotropic materials (their experimental Zener anisotropy ratio C_{44}/C' being close to 1) and thus the Voigt and Reuss bounds are close to each other (in fact they differ by less than 1 GPa). This averaging "uncertainty" is definitely below the measured ~5 GPa increase of G when adding 27% Ti to V, meaning that the experimental G, C_{44}, and C' are not consistent with each other. In order to solve this puzzle, further accurate measurements on the single-crystal and polycrystalline elastic parameters of V-based random alloys are needed.

The above theoretical values were obtained with the LDA-PBE scheme. We also investigated the effect of the fully self-consistent PBE method (PBE-PBE scheme) on the equation of state and elastic parameters of pure V and V-5Cr% and V-5Ti% alloys to find out whether this could change the theoretical results. We found that taking into account the gradient term in the one-electron potential during the self-consistent calculation changes, on the average, the three single-crystal elastic constants by ~15%. More importantly, both LDA-PBE and PBE-PBE schemes yield similar elastic parameter versus composition trends (with a mean deviation of ~30%) for the present systems, and thus the LDA-PBE scheme cannot account for the above-discussed deviation between theory and experiment.

Next we consider a few ternary alloys for which experimental elastic parameters are available. For V-Cr-Ti alloys, the general trends of bulk modulus, shear modulus, and Young's modulus are shown in Fig. 2. Our theoretical results are similar to the experimental values.[48,57–59] For instance, pure V exhibits larger bulk/shear modulus than that of V-4Cr-4Ti and V-4Cr-4Ti alloy has higher Young's modulus than that of V-5Cr-5Ti. On the other hand, the trends of the elastic moduli are slightly different in EMTO and former PAW[49] calculations. The deviation may be ascribed to the differences between the two theoretical studies. Namely, the present approach treats the problem of disorder within the CPA but does not allow atoms to relax. In the PAW calculations,[49] all atomic positions were allowed to relax but the solid solutions were modeled by a 250-atoms supercell with specific configuration (i.e., no configuration averaging was taken into account).

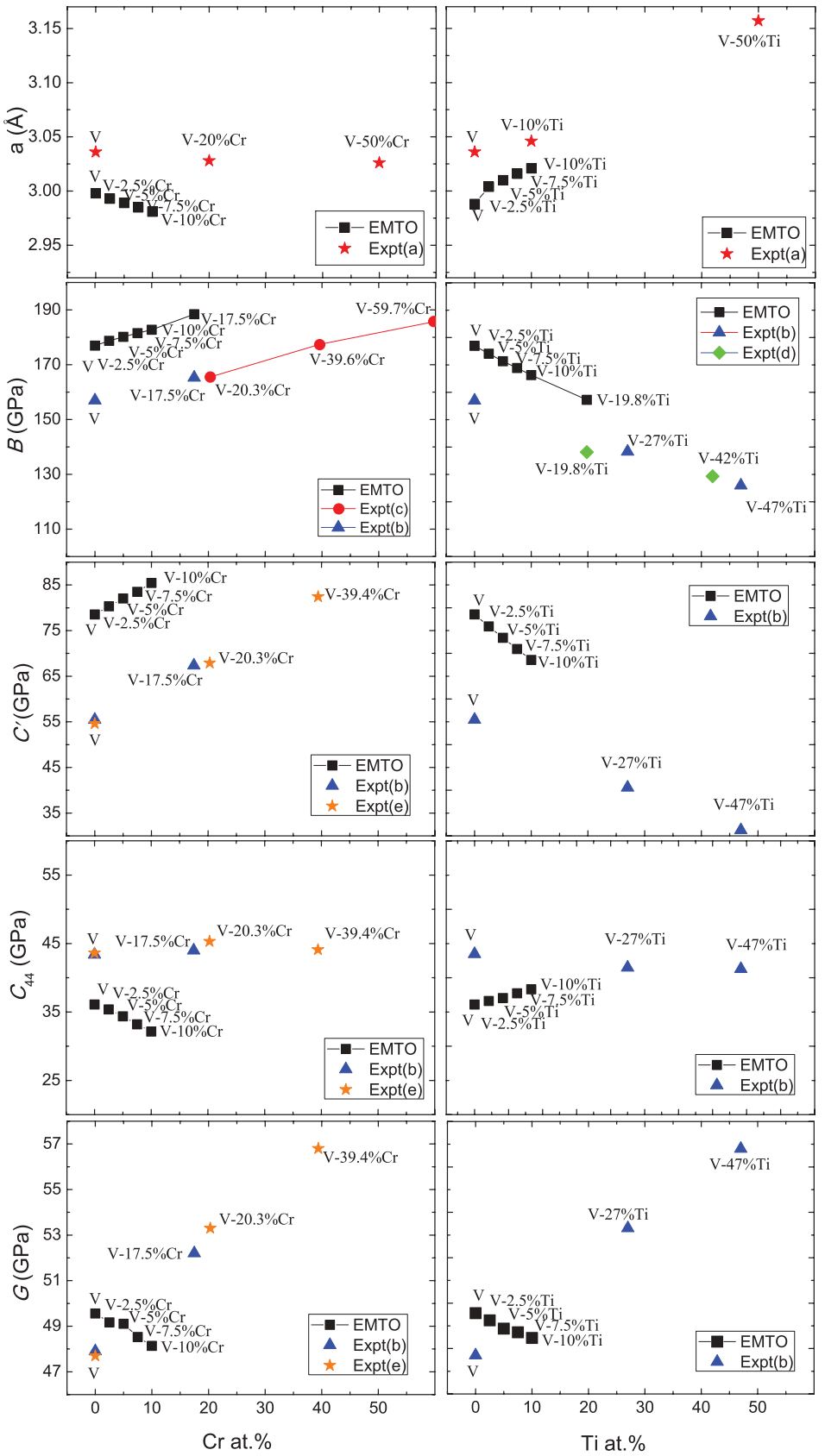

FIG. 1. (Color online) Theoretical (present results) and experimental lattice constants, bulk modulus, tetragonal shear elastic constant, C_{44} and shear modulus for binary bcc V-Cr and V-Ti alloys as a function of composition. Expt(a) from Ref. 54, Expt(b) from Ref. 53, Expt(c) Ref. 55, Expt(d) from Ref. 52, and Expt(e) from Ref. 56.

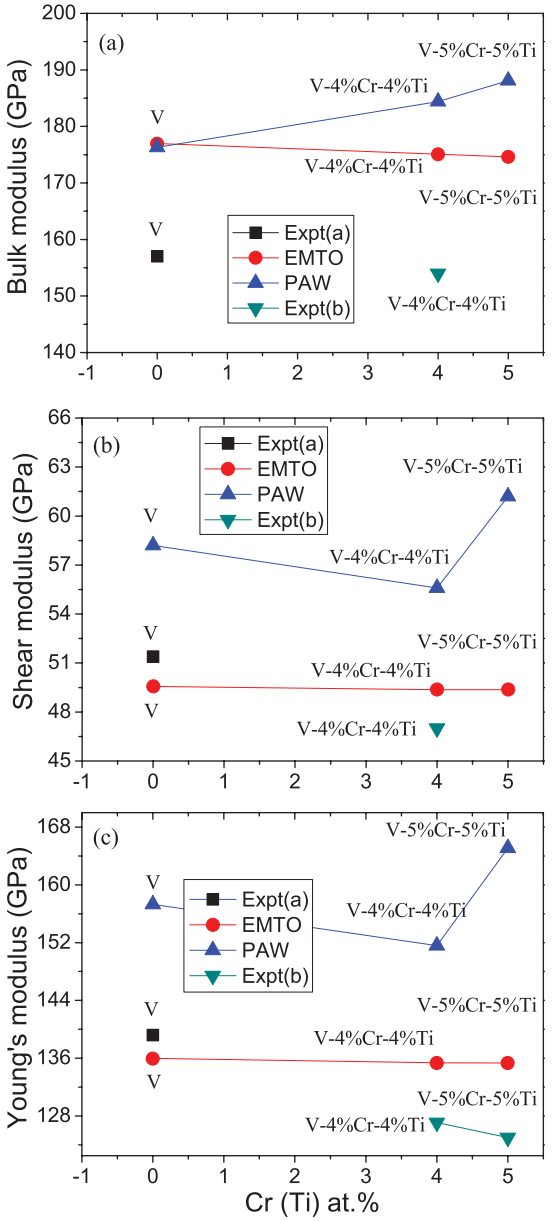

FIG. 2. (Color online) Theoretical (EMTO and PAW) and experimental polycrystalline bulk modulus, shear modulus, and Young's modulus for V-Cr-Ti alloys as a function of alloying elements. Expt(a) from Ref. 48 and Expt(b) from Ref. 57–59. The PAW results are from Ref. 49.

Based on the general agreement between the present theoretical predictions and the available experimental data from Figs. 1 and 2 and taking into account that the small discrepancies seen for binary alloys may very well be due to the experimental error bars, we conclude that our theoretical tool is able to describe the elastic properties of V-based alloys with sufficiently high accuracy.

C. Lattice constant and elastic parameters of V-Cr-Ti alloys

1. Lattice constants

Figure 3 shows the composition dependence of the lattice parameter of bcc V-Cr-Ti alloys. It is found that Cr addition shrinks the lattice parameter of pure V, whereas Ti enlarges

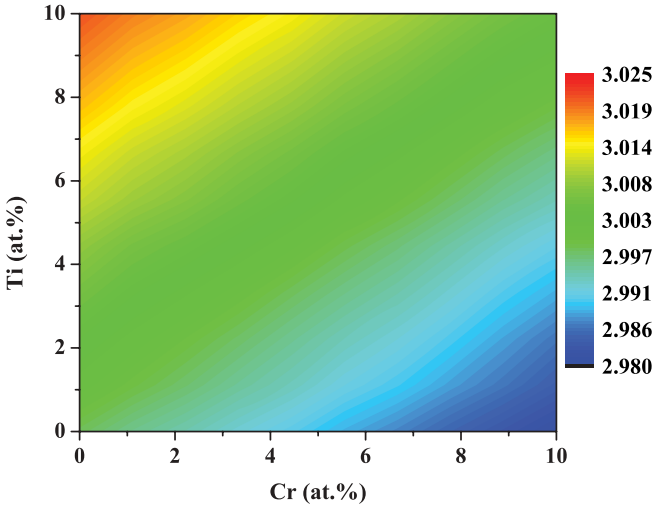

FIG. 3. (Color online) Theoretical lattice parameter (in Å) of bcc $V_{1-x-y}Cr_xTi_y$ ($0 \leqslant x,y \leqslant 0.1$) alloys as a function of Cr and Ti concentration.

it. This trend can be explained by the smaller atomic radius of bcc antiferromagnetic Cr (1.28 Å) and the larger one of hexagonal close-packed Ti (1.46 Å) as compared to that of bcc V (1.35 Å).[60] As a result of the two opposite alloying effects on the equilibrium volume, the lattice constants of V-Cr-Ti alloys are almost unchanged when equal amounts of Cr and Ti are introduced into V (alloys along the main diagonal in Fig. 3).

2. Single crystal elastic parameters

For each Cr and Ti concentration, the elastic constants of V-Cr-Ti alloys were calculated at the corresponding equilibrium lattice parameter from Fig. 3. In Fig. 4 we show the present theoretical single elastic constants C_{ij} (x,y) for bcc $V_{1-x-y}Cr_xTi_y$ as a function of Cr and Ti contents and in Table III we list the corresponding numerical values. At this point, we should mention that the actual accuracy of the present results is much lower than 0.01 GPa, which is the level of accuracy suggested by the figures in Table III (also Table IV). We estimated that 0.01 GPa is the numerical accuracy of our calculations for the cubic shear elastic constants. The lower absolute accuracy of our data is due to the fact that all our calculations were performed for completely random alloys, neglecting the local ordering and relaxation effects, using non-self-consistent PBE and full-charge density approach and neglecting the effect of temperature. Nevertheless, our elastic parameters from Table III (Table IV) may serve as a good reference for future *ab initio* studies performed within the above approximations.

We find that, in general, the effect of alloying on $C_{11}(x,y)$ is greater than that on $C_{12}(x,y)$ and $C_{44}(x,y)$. With the addition of Cr and Ti, $C_{11}(x,y)$ varies from ~258 GPa (corresponding to V-10%Ti, denoted by V-10Ti in the table) to ~297 GPa (V-10Cr), while the maximum changes in $C_{12}(x,y)$ and $C_{44}(x,y)$ are about 6 GPa. $C_{11}(x,y)$ increases with increasing x and decreases with increasing y, resulting in almost constant values along the diagonal (equiconcentration) region from Fig. 4. $C_{12}(x,y)$ varies between ~121 GPa (V-10Ti) and ~126 GPa (V-10Cr) and shows a weak dependence on the Cr content.

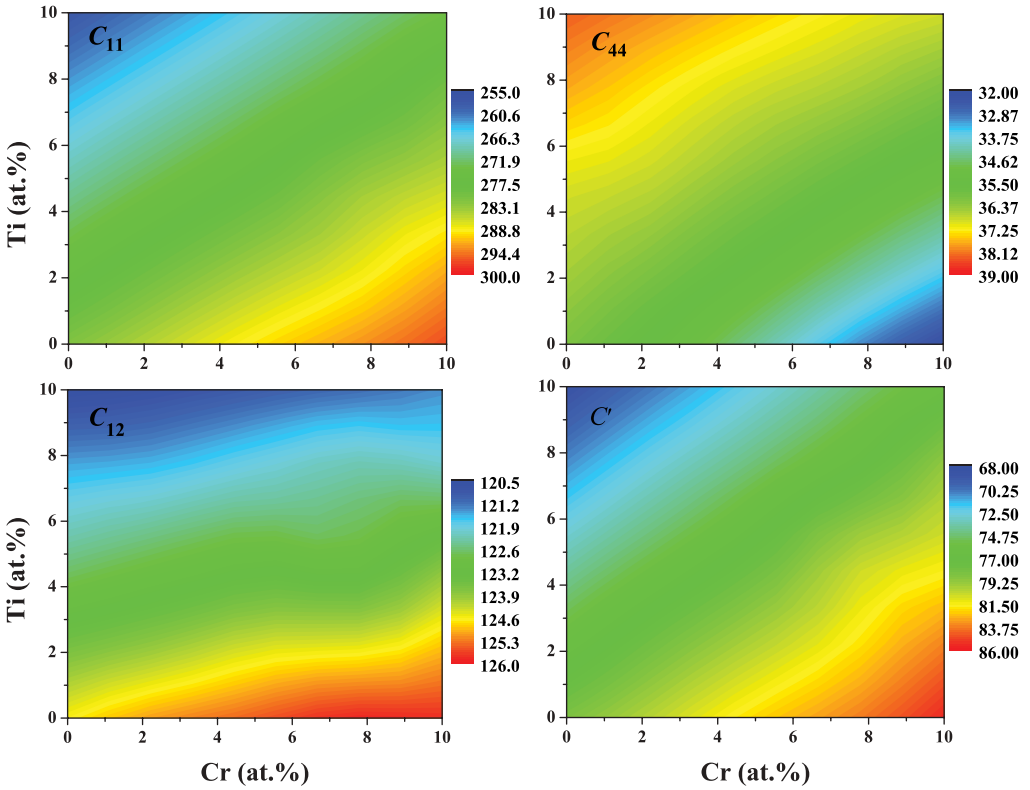

FIG. 4. (Color online) Theoretical single-crystal elastic constants (in GPa) for bcc $V_{1-x-y}Cr_xTi_y$ ($0 \leqslant x,y \leqslant 0.1$) alloys as a function of Cr and Ti concentrations.

The tetragonal shear elastic constant $C'(x,y)$ is often used to describe the structural stability of a cubic solid under tetragonal deformation.[61] As seen from Fig. 4, $C'(x,y)$ increases (decreases) with increasing Cr concentration (Ti concentration), and as a result of these opposite effects, $C'(x,y)$ for the alloys along the equicomposition diagonal region remains almost constant with increasing $x \approx y$. According to these trends, the V-Cr-Ti alloys become dynamically less stable with Ti addition and more stable with Cr addition.

The trends of $C'(x,y)$ can be explained using the following argument based on the volume effect. Since Ti expands the average volume per atom in V-Cr-Ti (Fig. 1), it also decreases the average bond strength and thus the ability of the alloy to resist the tetragonal shear. The introduction of Cr has the opposite effect. However, this simple picture obviously fails to explain the trends in the other single-crystal shear elastic constant $C_{44}(x,y)$. A more elaborated explanation for the calculated trends of $C'(x,y)$ is possible if we recall the correlation between the tetragonal elastic constant and the structural energy difference between the bcc and the face-centered-cubic (fcc) lattices.[50,62–64] According to that, large C' for the bcc phase corresponds to more stable bcc lattice compared to the fcc one. Referring to the crystal structure theory of transition metals,[65] it is known that in nonmagnetic solids with approximately three d electrons (i.e., close to bcc V) increasing (decreasing) d-occupation number stabilizes the bcc (fcc) phase. In the present case, Cr (Ti) addition increases (decreases) the d-occupation number and thus stabilizes (destabilizes) the bcc phase. As a consequence, Cr is expected to increase and Ti to decrease the tetragonal elastic constant. This trend is in perfect line with the *ab initio* results from Fig. 4.

In contrast to the tetragonal elastic constant, $C_{44}(x,y)$ exhibits similar trend as that of the lattice parameter plotted against Ti and Cr contents (Fig. 3). $C_{44}(x,y)$ decreases with Cr and increases with Ti addition to bcc V. Additional calculations yield larger C_{44} for elemental bcc Cr and bcc Ti than the one obtained for bcc V. Hence, neither the rule of mixing (i.e., linear interpolation between the results obtained for V and Cr and between those of V and Ti) nor the volume expansion can account for the predicted trend of $C_{44}(x,y)$ from Fig. 4.

Next we monitor the electronic structure of binary V-based alloys with the aim of finding an explanation for the unexpected (anomalous) composition dependence of $C_{44}(x,y)$. The elastic parameters are computed from the second-order derivation of total energy $E(\delta) = E(0) + a\delta^2 + O(\delta^4)$ with respect to the strain parameter δ. Since $\delta \leqslant 0.05$, the high-order terms $O(\delta^4)$ can be neglected and then we can write $C_{44} \sim \Delta E(\delta)/\delta^2$, where the $\Delta E(\delta) = E(\delta) - E(0)$ represents the change in total energy upon lattice distortion. According to the force theorem,[65] the total energy change can be approximated by the change of the one-electron energy ΔE_{one}, which in turn is determined by the density of state (DOS) calculated as a function of lattice distortion. In Fig. 5, we display the DOS for pure V, V-7.5Cr and V-7.5Ti alloys calculated in bcc phase (without lattice distortion) and with 5% distortion used to compute C_{44}. For pure V, there is a peak located approximately at -15 mRy below the Fermi level [marked by black dashed-dotted line in Fig. 5(a)]. Upon monoclinic distortion [Fig. 5(b)], this peak splits and shifts toward the

TABLE III. Theoretical lattice parameter (a in Å) and single-crystal elastic constants (in GPa) for bcc $V_{1-x-y}Cr_xTi_y$ ($0 \leqslant x,y \leqslant 0.1$) alloys as a function of Cr and Ti contents.

V-x%Cr-y%Ti	a	C'	C_{11}	C_{12}	C_{44}
V	2.998	78.54	281.72	124.63	36.09
V-2.5Cr	2.993	80.33	285.81	125.15	35.38
V-5Cr	2.989	82.06	289.59	125.48	34.37
V-7.5Cr	2.985	83.51	292.85	125.84	33.20
V-10Cr	2.981	85.44	296.66	125.79	32.15
V-2.5Ti	3.004	75.90	275.28	123.49	36.60
V-5Ti	3.010	73.40	269.21	122.40	37.03
V-7.5Ti	3.016	70.95	263.45	121.55	37.72
V-10Ti	3.021	68.58	257.71	120.55	38.32
V-2.5Cr-2.5Ti	2.999	77.97	279.76	123.82	36.11
V-2.5Cr-5Ti	3.005	75.38	273.49	122.72	36.76
V-2.5Cr-7.5Ti	3.011	72.93	267.53	121.67	37.27
V-2.5Cr-10Ti	3.017	70.53	261.76	120.70	37.94
V-4Cr-4Ti	3.000	77.61	278.56	123.34	36.16
V-5Cr-2.5Ti	2.995	79.75	283.72	124.23	35.47
V-5Cr-5Ti	3.001	77.38	277.78	123.02	36.24
V-5Cr-7.5Ti	3.007	74.83	271.64	121.97	36.85
V-5Cr-10Ti	3.012	72.45	265.81	120.92	37.53
V-7.5Cr-2.5Ti	2.991	81.46	287.22	124.30	34.62
V-7.5Cr-5Ti	2.996	79.92	282.71	122.87	35.68
V-7.5Cr-7.5Ti	3.002	76.81	275.88	122.25	36.51
V-7.5Cr-10Ti	3.008	74.42	269.97	121.12	37.17
V-10Cr-2.5Ti	2.986	83.34	291.44	124.77	33.76
V-10Cr-5Ti	2.992	81.02	285.66	123.62	35.03
V-10Cr-7.5Ti	2.998	79.34	280.81	122.13	36.05
V-10Cr-10Ti	3.004	76.36	274.07	121.35	36.90

TABLE IV. Theoretical polycrystalline elastic constants (in GPa), Poisson's ratio (ν), B/G ratio and Debye temperature (Θ, in K) for $V_{1-x-y}Cr_xTi_y$ ($0 \leqslant x,y \leqslant 0.1$) alloys as a function of Cr and Ti concentration.

V-x%Cr-y%Ti	B	G	B/G	E	ν	Θ
V	176.99	49.56	3.57	135.98	0.372	396.37
V-2.5Cr	178.70	49.47	3.61	135.87	0.373	395.71
V-5Cr	180.18	49.11	3.67	135.06	0.375	394.00
V-7.5Cr	181.51	48.53	3.74	133.67	0.377	391.39
V-10Cr	182.75	48.14	3.80	132.77	0.379	389.55
V-2.5Ti	174.09	49.24	3.54	134.99	0.371	395.74
V-5Ti	171.34	48.88	3.51	133.90	0.370	394.91
V-7.5Ti	168.85	48.72	3.47	133.32	0.368	394.87
V-10Ti	166.27	48.47	3.43	132.54	0.367	394.49
V-2.5Cr-2.5Ti	175.80	49.42	3.56	135.55	0.371	395.96
V-2.5Cr-5Ti	172.98	49.22	3.51	134.88	0.370	395.92
V-2.5Cr-7.5Ti	170.29	48.93	3.48	133.97	0.369	395.29
V-2.5Cr-10Ti	167.72	48.76	3.44	133.35	0.367	395.26
V-4Cr-4Ti	175.08	49.36	3.55	135.36	0.371	396.02
V-5Cr-2.5Ti	177.39	49.38	3.59	135.57	0.373	395.63
V-5Cr-5Ti	174.61	49.36	3.54	135.34	0.371	396.14
V-5Cr-7.5Ti	171.86	49.14	3.50	134.59	0.369	395.85
V-5Cr-10Ti	169.22	48.99	3.45	134.04	0.368	395.86
V-7.5Cr-2.5Ti	178.60	49.16	3.63	135.08	0.374	394.43
V-7.5Cr-5Ti	176.15	49.60	3.55	136.03	0.371	396.72
V-7.5Cr-7.5Ti	173.43	49.43	3.51	135.42	0.370	396.64
V-7.5Cr-10Ti	170.74	49.27	3.47	134.85	0.368	396.62
V-10Cr-2.5Ti	180.33	48.94	3.68	134.65	0.376	393.26
V-10Cr-5Ti	177.63	49.38	3.60	135.56	0.373	395.52
V-10Cr-7.5Ti	174.94	49.75	3.52	136.34	0.370	397.57
V-10Cr-10Ti	172.26	49.60	3.47	135.76	0.369	397.55

Fermi level, indicating a positive change in the one-electron energy, $\Delta E_{\text{one}} > 0$. Positive ΔE_{one} (in combination with the other energy terms) leads to positive C_{44} in bcc V. In V-Cr and V-Ti alloys the above scenario is slightly altered by alloying. Namely, the aforementioned DOS peak moves toward lower (higher) energy levels upon Cr (Ti) doping as compared to that in bcc V. This results in ΔE_{one}(V-7.5Cr) $< \Delta E_{\text{one}}$(V) $< \Delta E_{\text{one}}$(V-7.5Ti), suggesting C_{44}(V-7.5Cr) $< C_{44}$(V) $< C_{44}$(V-7.5Ti). Therefore, the electronic structure of bcc V provides an explanation for the anomalous C_{44} versus composition map (Fig. 4).

3. *Polycrystalline elastic properties*

The polycrystalline elastic parameters for bcc $V_{1-x-y}Cr_xTi_y$ alloys are listed in Table IV and shown in Fig. 6 as a function of composition. The bulk modulus varies between a minimum value of 166 GPa belonging to V-10Ti, and a maximum value of 183 GPa corresponding to V-10Cr. $B(x,y)$ follows the opposite trend obeyed by the lattice parameter (Fig. 1). Bulk modulus measures the resistance of material to uniform compression. Alloys with larger lattice constant correspond to lower average bond strength and thus they can be more easily compressed than those with smaller lattice constants. That explains why the bulk modulus of V-Cr-Ti alloys decreases with Ti and increases with Cr addition. The latter effect confers the excellent ductility properties of V-Cr-Ti alloys.

From Fig. 6, we can see that the variation of the shear modulus is very small within the present compositional map (about 2GPa). Along the diagonal region, $G(x,y)$ is relatively large, compared to the rest of the map, and slightly increases with increasing total solute concentration when $(x + y) > 0.1$–0.15. This particular saddle type of trend of $G(x,y)$ is due to the fact that $C_{44}(x,y)$ and $C'(x,y)$ show opposite variations with alloying (Fig. 4) and more specifically to the peculiar trend of $C_{44}(x,y)$ (see discussion in Sec. III C 2). The Young's modulus has similar composition dependence as that of the shear modulus, with V-10Cr-7.5Ti having the largest E value (136.7 GPa).

In the following we discuss the ductile/brittle behavior of V-Cr-Ti alloys, which is a crucial issue for the performance of structural materials. Previously, Pugh[23] proposed an approximate criterion for the ductile-brittle transition by means of the B/G value: A material is ductile when its B/G ratio is greater than 1.75; otherwise it is in brittle regime. The calculated values of B/G for all V-based alloys considered here are well above 1.75 (Table IV), suggesting that all of these alloys exhibit excellent ductile properties. In Fig. 6, we plotted the B/G ratio for the V-based alloys as a function of Cr and Ti concentration. We can see that alloys with large B/G ratios correspond to low Ti (<3 at.%) and high Cr (>6 at.%) concentration. The high-Ti-content (>7 at.%) alloys possess the lowest B/G ratio (<3.5) with a minimum around V-10Ti. Furthermore, we also find that the V-4Cr-4Ti alloy has marginally better ductility (in

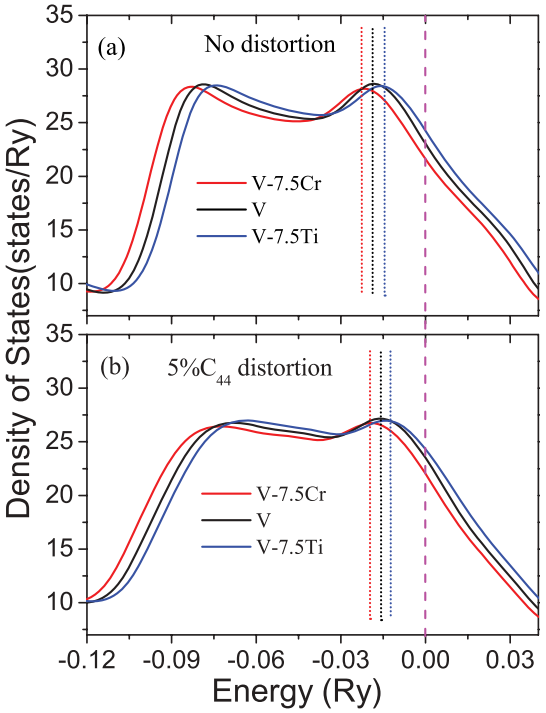

FIG. 5. (Color online) Density of states (DOS) for V, V-7.5Cr, and V-7.5Ti alloys in bcc lattice (a) and in C_{44}-type monoclinic distorted lattice (b) plotted for energies close to the Fermi level (marked by dashed line). The dash-dotted lines indicate the position of the DOS peak close to the Fermi.

term of B/G) than the V-5Cr-5Ti alloy. This is consistent with the experimental observation that at temperatures up to 400 °C V-4Cr-4Ti exhibits a larger uniform elongation (18%–23%) than V-5Cr-5Ti (14%–18%).[3]

The Poisson's ratio (ν) and elastic Debye temperature (Θ) are shown in Fig. 7 as a function of Cr and Ti contents. The Poisson's ratio has a similar trend as that of B/G. It has small values for high-Ti alloys and V-10Cr possesses the largest ν (0.379). Most V alloys have similar Debye temperatures (around 396 K) with a weak minimum (maximum) at V-10Cr (V-10Cr-7.5Ti) alloy. Based on this observation one would anticipate that lattice vibration effects have no significant impact on the phase diagram of V-Cr-Ti system within the considered compositional range.

We define the formation enthalpy of bcc $V_{1-x-y}Cr_xTi_y$ alloy as

$$\Delta H(x,y) = E(V_{1-x-y}Cr_xTi_y) - (1-x-y)E_{bcc}(V) - xE_{bcc}(Cr) - yE_{hcp}(Ti), \quad (8)$$

where all the energies were calculated at equilibrium volume and expressed per atom. $E_{bcc}(V)$, $E_{bcc}(Cr)$, and $E_{hcp}(Ti)$ are the total energies of bcc V, bcc Cr, and hcp Ti, respectively. According to Eq. (8), negative enthalpy of formation means that Cr, V, and Ti form a ternary V-Cr-Ti solid solution at low temperatures (static conditions). At finite temperature, we may approximate the Gibbs energy of formation of $V_{1-x-y}Cr_xTi_y$ alloys by $\Delta G \approx \Delta H - \Delta T S_{conf}$, where S_{conf} is the configuration entropy estimated as $S_{conf} = -k_B[x\ln(x) + y\ln(y) + (1-x-y)\ln(1-x-y)]$ (k_B is Boltzmann constant).

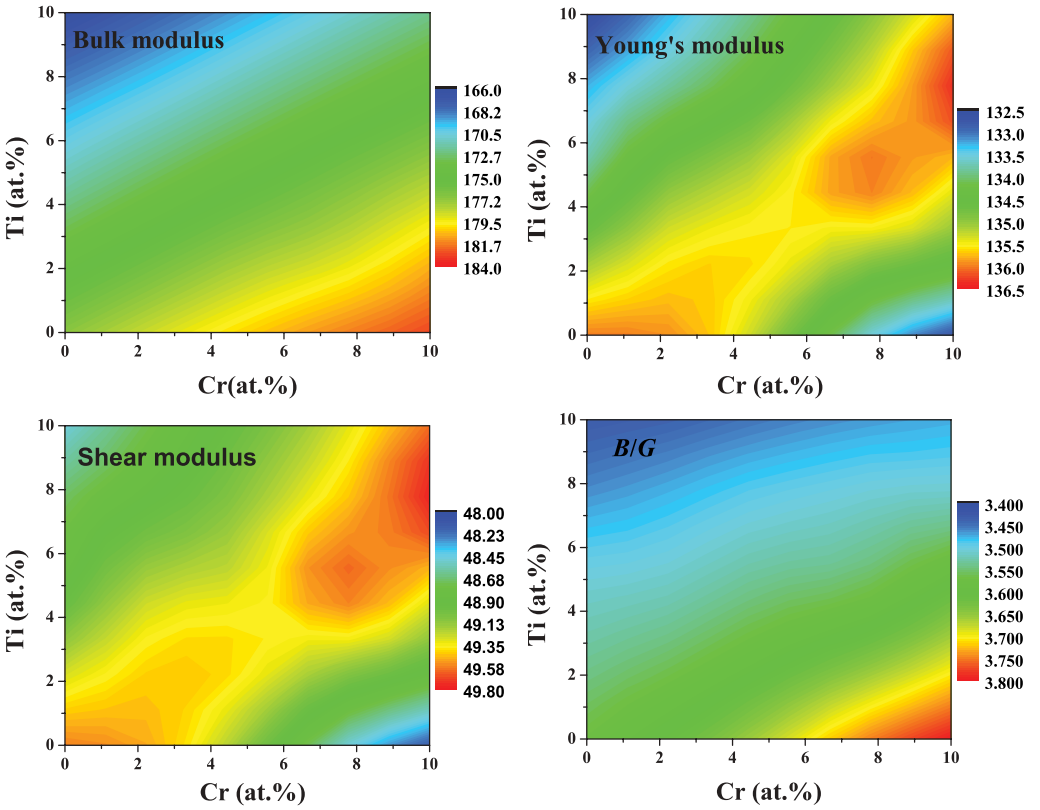

FIG. 6. (Color online) Theoretical polycrystalline elastic constants (in GPa) and B/G ratio for $V_{1-x-y}Cr_xTi_y$ ($0 \leqslant x,y \leqslant 0.1$) alloys as a function of Cr and Ti concentration.

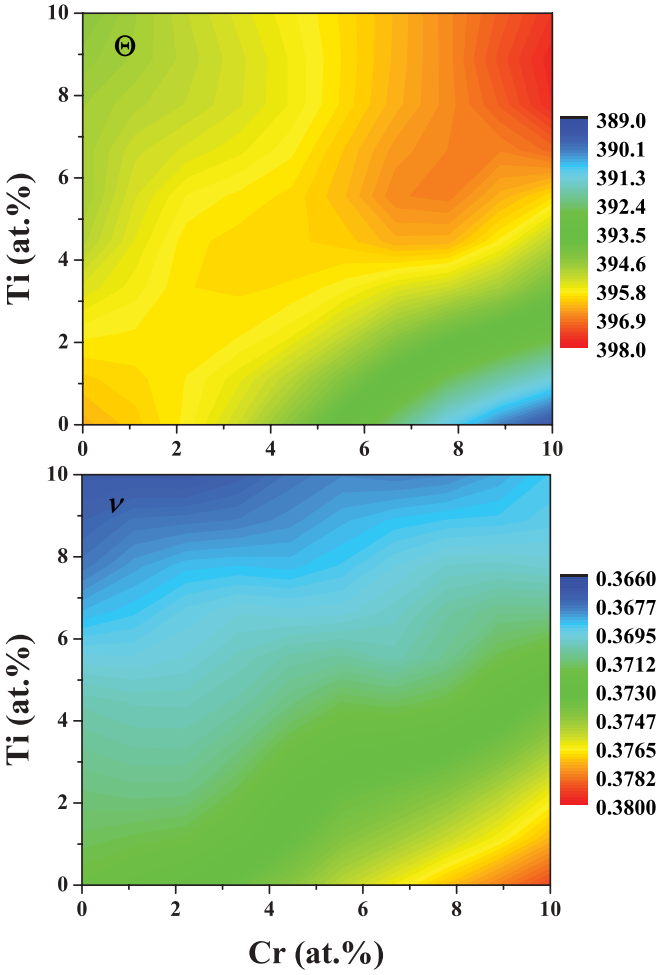

FIG. 7. (Color online) Theoretical Poisson's ratio (ν) and elastic Debye temperature (Θ, in K) for $V_{1-x-y}Cr_xTi_y$ ($0 \leqslant x,y \leqslant 0.1$) alloys as a function of Cr and Ti concentration.

The theoretical Gibbs energies of formation for V-based alloys at 0 K and 800 K are shown in Fig. 8. We find that at 0 K (top panel), V-Cr-Ti solid solutions can form with Ti concentration below 2–4 at.%, but solid solutions with larger Ti content are thermodynamically unstable. Considering the effect of temperature (bottom panel), we see that at 800 K most of ternary alloys become stable, and only compositions with low Cr (<2.5 at.%) and high Ti (>5 at.%) contents are unstable with respect to the considered standard states. These findings are consistent with the accepted ternary phase diagram of V-Cr-Ti system.[66] According to our predictions, the random solid solutions V-4Cr-4Ti and V-5Cr-5Ti become stable only above ~500 K. However, they might remain stable also at lower temperatures as a result of a significant short-range order effect not considered in the present study.

D. Solid solution hardening

The solid solution hardening (SSH) of V-Cr-Ti alloys as a function of Cr and Ti concentration may be estimated using the Labusch-Nabarro (LN) semiempirical model.[67–69] This model is often used to describe the hardening mechanism in alloys caused by solute atoms in an otherwise homogenous matrix.

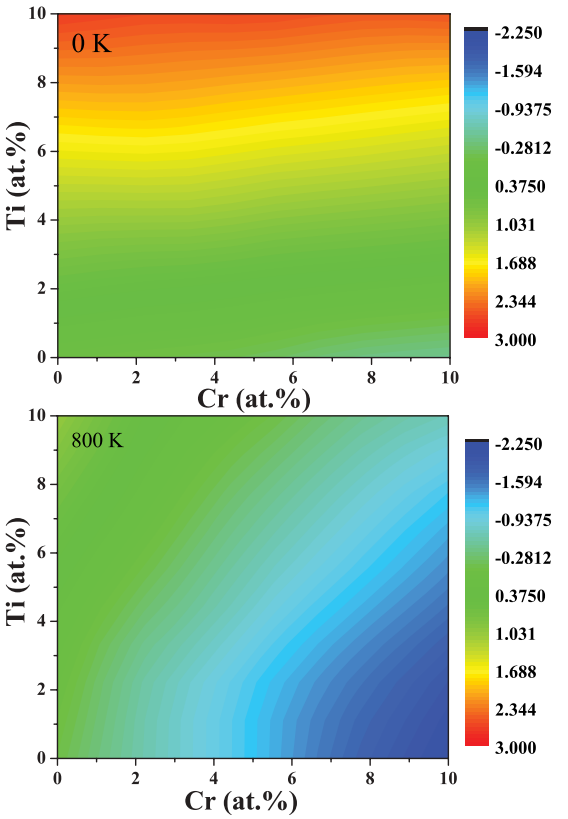

FIG. 8. (Color online) Theoretical (EMTO) Gibbs energy of formation for V-based alloys for temperature of 0 K and 800 K (in mRy per atom).

According to that, the SSH varies as

$$\Delta\tau = \text{const.} \times c^{2/3} \times \varepsilon_L^{4/3}, \tag{9}$$

where const. is a host-specific constant number (does not depend on c and the size of the misfit) the Fleischer parameter ε_L is expressed by

$$\varepsilon_L = [(\varepsilon'_{G-LN})^2 + (\alpha\varepsilon_b)^2]^{1/2} \quad \text{with}$$
$$\varepsilon'_{G-LN} = \varepsilon_G/(1 + 0.5\,|\varepsilon_G|), \tag{10}$$

with α being a parameter (in the present application we adopted $\alpha = 10$), and ε_b and ε_G are the volume and modulus misfit parameters, respectively. These parameters can be obtained from the composition-dependent lattice constant and shear modulus of binary $V_{1-c}Cr_c$ and $V_{1-c}Ti_c$ alloys, viz.,

$$\varepsilon_b = [\delta(b)/\delta c]/b(0) \quad \text{and} \quad \varepsilon_G = [\delta(G)/\delta c]/G(0), \tag{11}$$

where b is Burger's vector, G is shear modulus, and c is the atomic fraction of the solute atom.

The theoretical misfit parameters calculated for V-7.5Cr and V-7.5Ti are listed in Table V. According to these numbers,

TABLE V. Theoretical volume and elastic misfit parameters and Fleischer parameter for bcc V-7.5Cr and V-7.5Ti alloys.

	ε_b	ε_G	ε_{G-LN}	ε_L
V-7.5Cr	–0.056	–0.277	–0.243	0.614
V-7.5Ti	–0.079	–0.226	–0.203	0.818

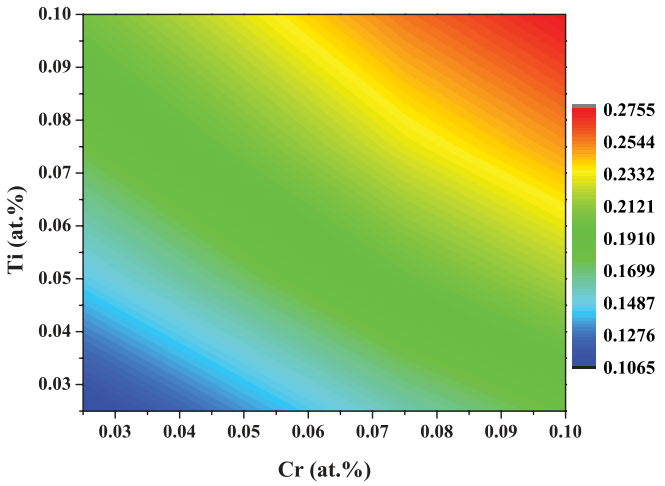

FIG. 9. (Color online) Solid solution hardening [units of const. in (9)] in ternary $V_{1-x-y}Cr_xTi_y$ ($0 \leqslant x,y \leqslant 0.1$) alloys as a function of Cr and Ti concentrations.

both Cr and Ti induce SSH in V, but Ti has slightly larger strengthening effect than Cr. These theoretical predictions are in line with the observations.[70,71]

Here we estimate the SSH of ternary V-Cr-Ti alloys by simply summing the effects obtained for the V-Cr and V-Ti binary alloys. The total theoretical SSH map is shown in Fig. 9. One can see that for total solute concentration below ~10 at.%, the SSH has relatively low value (as compared to the dilute alloys). Obviously, the SSH increases more with Ti content than with Cr content as a result of the larger misfit parameters obtained for a Ti-doped system.

Experimental works usually focus on the effect of the solute atoms on the DBTT. The DBTT has been shown to be related to yield strength.[72] The yield strength in turn includes three parts: lattice friction strengthening (Peierls stress), solid solution strengthening (SSH), and grain boundary strengthening that can be estimated by Hall-Petch relationship. In the following, using our calculated results obtained for the elastic and misfit parameters, we try to explain the observed variation of the DBTT with composition.[2]

As shown in Fig. 6, along the main diagonal, the V-Cr-Ti alloys with high ($x + y$) (above ~0.15) have the highest shear modulus, indicating that these alloys possess the highest Peierls stress. Alloys outside of this region have slightly lower Peierls stress. Combining this result with the SSH from Fig. 9, we arrive at the conclusion that the yield stress should increase with both Cr and Ti addition, and this increase should be more pronounced along the main diagonal ($x \approx y$). Hence, our results suggest that the DBTT should show nearly symmetric composition dependence (as a function of Cr and Ti contents) with a maximum for the equiconcentration alloys with ($x + y$) larger than 0.1–0.15. A very similar DBTT map was established from experimental measurements.[2] Namely, Chung *et al.*[1] found that the V-Cr-Ti alloys with total concentration of Cr and Ti below 10% show the lowest DBTT, and DBTT increases with increasing the total concentration of Cr and Ti (above 10 at.%), which is consistent with our prediction.

IV. CONCLUSIONS

Using the EMTO method in combination with the CPA, we have investigated the elastic properties of V-based alloys as a function of Ti and Cr concentration. Chromium addition decreases and titanium addition increases the lattice constant of bcc vanadium. As a consequence, the lattice constant of V-Cr-Ti alloys remains unchanged when equal amounts of Cr and Ti are introduced into V. The two cubic shear elastic constants follow opposite trends, which results in a local maximum in the shear and Young's moduli for the equi-concentration alloys. The anomalous composition dependence of C_{44} has been explained using the electronic structure of bcc V.

All V-based alloys exhibit excellent ductile behavior shown by the large B/G values. The addition of Cr increases the bulk modulus and the ductility of V-based alloys. At 0 K, the solid solutions can form with low Ti concentration, but at 800 K most compositions considered here become stable and only alloys with high Ti concentration remain unstable. Both Cr and Ti enhance the solid solution hardening of V-based alloys but Ti has larger strengthening effect than Cr. The SSH of the ternary alloys increases with increasing the total Cr and Ti concentration. We have used our theoretical data to explain the changes of DBTT of V-Cr-Ti alloys as a function of Cr and Ti concentration. The present results offer a consistent starting point for further theoretical modeling of the elastic and micromechanical properties of V-based alloys.

ACKNOWLEDGMENTS

The Swedish Research Council, the Swedish Steel Producers' Association, the European Research Council, the China Scholarship Council, and the Hungarian Scientific Research Fund (Research Project No. OTKA 84078) and the National Magnetic Confinement Fusion Program of China (2011GB108007) are acknowledged for financial support.

*Corresponding author: xiaoqli@kth.se; zhaojj@dlut.edu.cn

[1] H. M. Chung, B. A. Loomis, and D. L. Smith, J. Nucl. Mater. **239**, 139 (1996).

[2] H. Matsui, K. Fukumoto, D. L. Smith, H. M. Chung, W. vanWitzenburg, and S. N. Votinov, J. Nucl. Mater. **233**, 92 (1996).

[3] D. L. Smith, H. M. Chung, H. Matsui, and A. F. Rowcliffe, Fusion Eng. Des. **41**, 7 (1998).

[4] R. J. Kurtz, K. Abe, V. M. Chernov, V. A. Kazakov, G. E. Lucas, H. Matsui, T. Muroga, G. R. Odette, D. L. Smith, and S. J. Zinkle, J. Nucl. Mater. **283**, 70 (2000).

[5] D. L. Smith, M. C. Billone, and K. Natesan, Int. J. Refract. Met. Hard Mater. **18**, 213 (2000).

[6] T. Muroga, T. Nagasaka, K. Abe, V. M. Chernov, H. Matsui, D. L. Smith, Z. Y. Xu, and S. J. Zinkle, J. Nucl. Mater. **307**, 547 (2002).

[7]H. M. Chung, B. A. Loomis, and D. L. Smith, J. Nucl. Mater. **212**, 804 (1994).

[8]H. D. Rohrig, J. R. DiStefano, and L. D. Chitwood, J. Nucl. Mater. **258**, 1356 (1998).

[9]H. Tsai, T. S. Bray, H. Matsui, M. L. Grossbeck, K. Fukumoto, J. Gazda, M. C. Billone, and D. L. Smith, J. Nucl. Mater. **283**, 362 (2000).

[10]K. Natesan, W. K. Soppet, and M. Uz, J. Nucl. Mater. **258**, 1476 (1998).

[11]K. Fukumoto, T. Morimura, T. Tanaka, A. Kimura, K. Abe, H. Takahashi, and H. Matsui, J. Nucl. Mater. **239**, 170 (1996).

[12]D. S. Gelles, P. M. Rice, S. J. Zinkle, and H. M. Chung, J. Nucl. Mater. **258**, 1380 (1998).

[13]S. N. Votinov, M. I. Solonin, Y. I. Kazennov, V. P. Kondratjev, A. D. Nikulin, V. N. Tebus, E. O. Adamov, S. E. Bougaenko, Y. S. Strebkov, A. V. Sidorenkov, V. B. Ivanov, V. A. Kazakov, V. A. Evtikhin, I. E. Lyublinski, V. M. Trojanov, A. E. Rusanov, V. M. Chernov, and G. A. Birgevoj, J. Nucl. Mater. **233**, 370 (1996).

[14]H. M. Chung and D. L. Smith, J. Nucl. Mater. **258**, 1442 (1998).

[15]H. M. Chung, B. A. Loomis, and D. L. Smith, Fusion Eng. Des. **29**, 455 (1995).

[16]E. G. Donahue, G. R. Odette, and G. E. Lucas, J. Nucl. Mater. **283**, 518 (2000).

[17]B. G. Gieseke, C. O. Stevens, and M. L. Grossbeck, J. Nucl. Mater. **233**, 488 (1996).

[18]M. M. Potapenko, V. A. Drobishev, V. Y. Filkin, I. N. Gubkin, V. V. Myasnikov, A. D. Nikulin, E. N. Shingarev, G. P. Vedernikov, S. N. Votinov, V. S. Zurabov, and A. B. Zolotarev, J. Nucl. Mater. **233**, 438 (1996).

[19]P. M. Rice and S. J. Zinkle, J. Nucl. Mater. **258**, 1414 (1998).

[20]S. H. Jhi, J. Ihm, S. G. Louie, and M. L. Cohen, Nature **399**, 132 (1999).

[21]D. G. Clerc and H. M. Ledbetter, J. Phys. Chem. Solids **59**, 1071 (1998).

[22]X. Jiang, J. J. Zhao, and X. Jiang, Comput. Mater. Sci. **50**, 2287 (2011).

[23]S. F. Pugh, Philos. Mag. **45**, 823 (1954).

[24]D. G. Pettifor, Mater. Sci. Technol. **8**, 345 (1992).

[25]O. K. Andersen, O. Jepsen, and G. Krier, in *Lectures on Methods of Electronic Structure Calculations*, edited by V. Kumar, O. K. Andersen, and A. Mookerjee (World Scientific, Singapore, 1994), p. 63.

[26]L. Vitos, Phys. Rev. B **64**, 014107 (2001).

[27]L. Vitos, H. L. Skriver, B. Johansson, and J. Kollár, Comput. Mater. Sci. **18**, 24 (2000).

[28]P. Hohenbery and W. Kohn, Phys. Rev. B **136**, 864 (1964).

[29]J. P. Perdew and Y. Wang, Phys. Rev. B **45**, 13244 (1992).

[30]J. P. Perdew, K. Burke, and M. Ernzerhof, Phys. Rev. Lett. **77**, 3865 (1996).

[31]J. Kollár, L. Vitos, and H. L. Skriver, in *Electronic Structure and Physical Properties of Solids: the uses of the LMTO method*, edited by H. Dreyssé, Lectures Notes in Physics (Springer-Verlag, Berlin, 2000), p. 85.

[32]M. Ropo, K. Kokko, and L. Vitos, Phys. Rev. B **77**, 195445 (2008).

[33]M. Asato, A. Settels, T. Hoshino, T. Asada, S. Blugel, R. Zeller, and P. H. Dederichs, Phys. Rev. B **60**, 5202 (1999).

[34]B. L. Gyorffy, Phys. Rev. B **5**, 2382 (1972).

[35]A. Taga, L. Vitos, B. Johansson, and G. Grimvall, Phys. Rev. B **71**, 014201 (2005).

[36]L. Vitos, I. A. Abrikosov, and B. Johansson, Phys. Rev. Lett. **87**, 156401 (2001).

[37]L. Vitos, *Computational Quantum Mechanicals for Materials Engineers* (Springer-Verlag, London, 2007).

[38]O. K. Andersen, C. Arcangeli, R. W. Tank, T. Saha-Dasgupta, G. Krier, O. Jepsen, and I. Dasgupta, in *Tight-Binding Approach to Computational Materials Science*, edited by P. E. A. Turchi, A. Gonis, and L. Colombo, MRS Symposia Proceedings No. 491 (Materials Research Society, Pittsburgh, 1998), pp. 3-34.

[39]L. Huang, L. Vitos, S. K. Kwon, B. Johansson, and R. Ahuja, Phys. Rev. B **73**, 104203 (2006).

[40]J. Zander, R. Sandström, and L. Vitos, Comput. Mater. Sci. **41**, 86 (2007).

[41]B. Magyari-Köpe, G. Grimvall, and L. Vitos, Phys. Rev. B **66**, 064210 (2002).

[42]B. Magyari-Köpe, L. Vitos, and G. Grimvall, Phys. Rev. B **70**, 052102 (2004).

[43]L. Vitos, P. A. Korzhavyi, and B. Johansson, Nat. Mater **2**, 25 (2003).

[44]V. L. Moruzzi, J. F. Janak, and K. Schwarz, Phys. Rev. B **37**, 790 (1988).

[45]E. K. Delczeg-Czirjak, L. Delczeg, M. Ropo, K. Kokko, M. P. J. Punkkinen, B. Johansson, and L. Vitos, Phys. Rev. B **79**, 085107 (2009).

[46]R. Hill, Proc. Phys. Soc., London, Sect. A **65**, 349 (1952).

[47]H. M. Ledbetter, J. Appl. Phys. **44**, 1451 (1973).

[48]D. I. Bolef, R. E. Smith, and J. G. Miller, Phys. Rev. B **3**, 4100 (1971).

[49]X. Li, C. Zhang, J. Zhao, and B. Johansson, Comput. Mater. Sci. **50**, 2727 (2011).

[50]P. Söderlind, O. Eriksson, J. M. Wills, and A. M. Boring, Phys. Rev. B **48**, 5844 (1993).

[51]M. J. Mehl and D. A. Papaconstantopoulos, Phys. Rev. B **54**, 4519 (1996).

[52]J. T. Lenkkeri, J. Phys. F **10**, 611 (1980).

[53]K. W. Katahara, M. H. Manghnani, and E. S. Fisher, J. Phys. F **9**, 773 (1979).

[54]D. O. Van Ostenburg, D. J. Lam, H. D. Trapp, and D. E. MacLeod, Phys. Rev. **128**, 1550 (1962).

[55]J. T. Lenkkeri and E. E. Lahteenkorva, J. Phys. F **8**, 1643 (1978).

[56]P. Bujard and E. Walker, Solid State Commun. **43**, 65 (1982).

[57]B. K. Kardashev, V. M. Chernov, O. A. Plaskin, V. A. Stepanov, and L. P. Zavialski, J. Alloys Compd. **310**, 102 (2000).

[58]D. L. Smith, H. M. Chung, B. A. Loomis, H. Matsui, S. Votinov, and W. Vanwitzenburg, Fusion Eng. Des. **29**, 399 (1995).

[59]B. Kardashev and V. Chernov, Phys. Solid State **50**, 854 (2008).

[60]C. Kittle, *Introduction to Solid State Physics* (Wiley, New York, 1986), p. 23.

[61]J. Wang, S. Yip, S. R. Phillpot, and D. Wolf, Phys. Rev. Lett. **71**, 4182 (1993).

[62]J. M. Wills, O. Eriksson, P. Söderlind, and A. M. Boring, Phys. Rev. Lett. **68**, 2802 (1992).

[63]P. J. Craievich, J. M. Sanchez, R. E. Watson, and M. Weinert, Phys. Rev. B **55**, 787 (1997).

[64]P. J. Craievich, M. Weinert, J. M. Sanchez, and R. E. Watson, Phys. Rev. Lett. **72**, 3076 (1994).
[65]H. L. Skriver, Phys. Rev. B **31**, 1909 (1985).
[66]M. Enomoto, J. Phase Equilib. **13**, 195 (1992).
[67]R. L. Fleischer, Acta Metall. **11**, 203 (1963).
[68]F. R. N. Nabarro, Philos. Mag. **35**, 613 (1977).
[69]R. Labusch, Acta Metall. **20**, 917 (1972).
[70]N. Iwao, T. Kainuma, T. Suzuki, and R. Watanabe, J. Less Common Met. **83**, 205 (1982).
[71]C. Owen, W. Spitzig, and O. Buck, Metall. Mater. Trans. A **18**, 1593 (1987).
[72]B. Hwang, T.-H. Lee, and S.-J. Kim, Met. Mater. Int. **16**, 905 (2010).